Invariant Error Dynamics Controller for a 6-dof Electrohydraulic Stewart Platform

Ioannis Davliakos and Evangelos Papadopoulos [1]

National Technical University of Athens, Department of Mechanical Engineering
15780 Athens Greece
e-mail: {gdavliak | egpapado@central.ntua.gr}

Abstract. The study of the invariant error dynamics controller for a six-degrees-of-freedom (dof) electrohydraulic Stewart platform is presented. Rigid body and electrohydraulic models, including servovalve dynamics are employed. Friction is also included in the mechanical model. The developed controller employs the dynamic and hydraulic model of the system and yields the six servovalve input current vector, in analytical form. Using mechanism inverse kinematics, the desired Cartesian trajectories yield desired actuator length trajectories. Simulations with typical desired trajectories are presented and a good performance of the controller is obtained.

1 Introduction

Stewart platform type (Stewart, 1965-66) parallel manipulators have been studied in their kinematics (see, e.g., Shim et al., 1997, Liu et al., 2000, Gao et al., 2005) and dynamics (Lebret et al., 1993, Tsai, 1999, 2000). Although electrohydraulic Stewart platforms have been used in the past, even commercially–mainly in aircraft simulations, not much published work on their dynamics and control (see, e.g., Li and Salcudean, 1997, Sirouspour and Salcudean, 2000, Kim et al., 2000) exists.

Hydraulics science combined with controls, has given new thrust to hydraulics applications. The main reasons why hydraulics are preferred to electromechanical drives in some industrial and mobile applications, include their ability to produce large forces at high speeds, their high durability and stiffness, and their rapid response (Merritt, 1967). Hydraulic systems differ from electromechanical ones, in that the force or torque output is not proportional to actuator current and therefore, hydraulic actuators cannot be modeled as force /torque sources. As a result, controllers that have been designed for robot control, assuming the capability of setting actuator force/torque, cannot be used here.

Control techniques are used to compensate for the nonlinearities of electrohydraulic servosystems. Nonlinear adaptive control techniques for hydraulic servosystems have been proposed by researchers assuming linearization (Garagic and Srinivasan, 2004) and backstepping (Sirouspour and Salcudean, 2001), approaches. The modelling of an experimental hydraulic robot arm and the implementation of a model-based motion controller that compensates for dynamic

[1] Support by the EPAN Cooperation Program 4.3.6.1 (Greece-Poland) of the Hellenic General Secretariat for Research and Technology and the NTUA Senator Committee of Basic Research Programme "Protagoras", R.C. No. 10, is acknowledged.

forces have been presented by Honegger and Corke (2001). A tracking controller for electrohydraulic servosystems has been developed (Davliakos and Papadopoulos, 2005) including a fast model-based force tracking loop.

Nguyen et al. (1992) have developed a joint-space adaptive control scheme applied to an electromechanically driven Stewart platform-based manipulator, using the Lyapunov direct method under the assumption that Stewart platform motion was slow compared to the controller adaptation rate. Also, Kim and Lee (1998), studied and applied a high speed tracking control of a 6-6 electric Stewart platform, using an enhanced sliding mode control approach.

Further, the modeling and control of an inverted, ceiling-mounted electrohydraulically driven Stewart platform has been researched (Li and Salcudean, 1997), using the virtual work principle and a pressure feedback control approach. Extended work of the same mechanism has been studied and applied (Sirouspour and Salcudean, 2000), in which the Lyapunov analysis approach has been used for a nonlinear controller. A robust tracking control design for a 6-dof hydraulically driven Stewart type mechanism has been developed (Kim et al., 2000) and has been achieved, using two types of controllers, which were based on Lyapunov analysis.

In this paper, a simulation of the invariant error dynamics controller for a 6-dof electrohydraulic Stewart platform is developed. Dynamic models are presented and they describe the rigid body equations of motion and the hydraulic dynamics of the main elements. Friction is included in the model. The developed control scheme employs the dynamic and hydraulic model of the system and yields the six servovalve input current vector, in analytical form. Using mechanism inverse kinematics, the desired Cartesian trajectories yield desired actuator length trajectories. Simulations with typical desired trajectories are presented and a good performance of the controller is obtained. The approach can be further extended to hydraulic manipulator and simulator control.

2 Dynamic Modelling of the Six - Dof Electrohydraulic Stewart Platform

In this section, the dynamic model of a 6-dof electrohydraulic Stewart platform servomechanism (Stewart, 1965-66) is developed. This is a six dof closed kinematic chain mechanism consisting of a fixed base and a movable platform with six linear actuators supporting it. The mechanism is illustrated schematically in Figure 1.

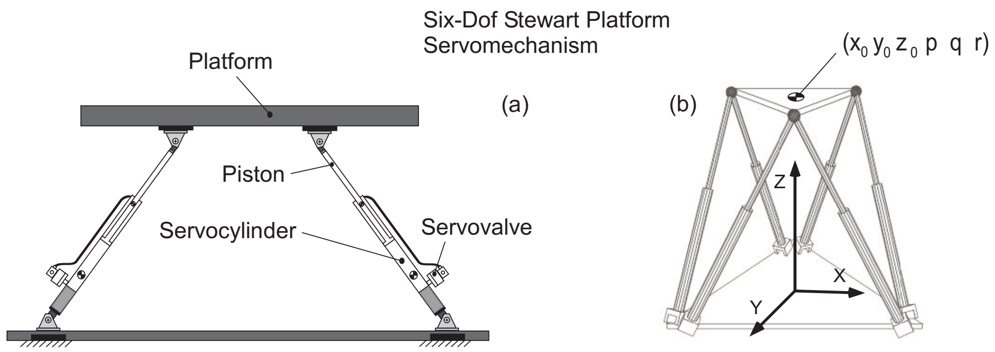

Figure 1. (a) Drawing two of the six servoactuators, (b) Schematic view of a six-dof Stewart Platform.

A full servosystem model includes the moving mass equation of motion. This system provides a relation between the actuator torques/forces and the resulting motion. The equation of motion for the Stewart platform system is derived applying a Lagrangian formulation and is written as

$$\mathbf{M}(\boldsymbol{l})\ddot{\boldsymbol{l}} + \boldsymbol{V}(\boldsymbol{l},\dot{\boldsymbol{l}}) + \boldsymbol{G}(\boldsymbol{l}) + \boldsymbol{F}_{\boldsymbol{fr}}(\dot{\boldsymbol{l}}) = \boldsymbol{F}_{\boldsymbol{p}} \tag{1}$$

where $\boldsymbol{l}$ is the 6×1 displacement vector of the mechanism actuators, $\mathbf{M}(\boldsymbol{l})$ is the 6×6 positive definite mass matrix of the system, the 6×1 vector $\boldsymbol{V}(\boldsymbol{l},\dot{\boldsymbol{l}})$ represents forces/torques arising from centrifugal and Coriolis forces, the 6×1 vector $\boldsymbol{G}(\boldsymbol{l})$ represents torques due to gravity, $\boldsymbol{F}_{\boldsymbol{fr}}(\dot{\boldsymbol{l}})$ is the 6×1 vector of the forces/torques due to friction and $\boldsymbol{F}_{\boldsymbol{p}}$ is the 6×1 vector of the actuator forces $F_{\mathrm{p,j}}$, $j=1,2,...,6$ (see section 3).

A number of methods exists, that model the friction vector $\boldsymbol{F}_{\boldsymbol{fr}}(\dot{\boldsymbol{l}})$, (Helouvry et al., 1994). A widely used method computes friction vector, the elements of which are given by,

$$F_{fr}(\dot{l}_j) = \begin{cases} f_{C,j}\,\mathrm{sgn}(\dot{l}_j) + b_j\dot{l}_j\,, & \dot{l}_j \neq 0 \\ f_{ext,j}\,, & \left|f_{ext,j}\right| < f_{s,j}\,,\ \dot{l}_j = 0,\ \ddot{l}_j = 0 \\ f_{s,j}\,\mathrm{sgn}(f_{ext,j}), & \left|f_{ext,j}\right| > f_{s,j}\,,\ \dot{l}_j = 0,\ \ddot{l}_j \neq 0 \end{cases} \tag{2}$$

where l_{j} is the j actuator displacement, b_{j}, $f_{C,j}$, $f_{ext,j}$, $f_{s,j}$ are the j parameters of viscous friction coefficient, Coulomb friction, external force and breakaway force, which is the limit between static and kinetic friction, respectively, for $j=1,2,...,6$, and sgn is the sign function.

If the motion of the platform is specified in the 6-dof Cartesian space (x_0, y_0, z_0, p, q, r), where x_0, y_0, z_0 are the Cartesian generalized coordinates of the platform center of mass (cm) and p, q, r are the Euler angles, then inverse kinematics must be used to determine the required leg lengths that correspond to the desired motion.

3 Electrohydraulic Servosystem Modelling

In this section, the dynamic modelling of high performance electrohydraulic servocylinders is presented briefly. An electrohydraulic servosystem consists of a servomechanism, including servovalves, servoactuators, controllers, mechanical loads and a hydraulic power supply. Next, simple models of major components are described.

An ideal single rod hydraulic cylinder is described by

$$Q_r = A_r\dot{l}\,,\quad r=1,2 \tag{3a}$$

$$p_1A_1 - p_2A_2 = F_{\mathrm{p}} \tag{3b}$$

where Q_r are the flows through its two chamber ports, p_1, p_2 are the chamber pressures, A_1 is the piston side area, A_2 is the rod side area, l is the piston displacement and F_{p} is the piston output force. A real cylinder model also includes chamber oil compressibility, chamber leakages and other effects. However, these can be neglected at an initial stage.

A typical hydraulic servovalve consists of four symmetric and matched servovalve orifices making up a four-legged flow path of four nonlinear resistors, modulated by the input voltage.

Thereby, the servovalve is modeled as the hydraulic equivalent of a Wheatstone bridge, see Figure 2. When the servovalve input current is positive, $i > 0$, flow passes through the orifices 1 and 3 (path $P \rightarrow A \rightarrow B \rightarrow T$), and flow leakages exist in the valve orifices 2 and 4. Respectively, when the servovalve input current is negative, $i < 0$, flow passes through the path $P \rightarrow B \rightarrow A \rightarrow T$, and flow leakages exist in the valve orifices 1 and 3. This model is described by

$$Q_{v1} = f_1(i)\sqrt{p_s - p_1}, \; Q_{v2} = f_2(i)\sqrt{p_s - p_2}, \; Q_{v3} = g_1(i)\sqrt{p_2 - p_T}, \; Q_{v4} = g_2(i)\sqrt{p_1 - p_T} \quad (4)$$

where p_s and p_T are the power supply and return pressure of the servosystem, respectively, i is the servovalve motor current (control command), $f_1(i)$, $f_2(i)$, $g_1(i)$ and $g_2(i)$ are servovalve nonlinear orifice conductances, functions of the servovalve motor current. Because of servovalve symmetry, the current functions are given by

$$f_1(i) = g_1(i) = f_2(-i), \qquad f_2(i) = g_2(i) = f_1(-i) \quad (5)$$

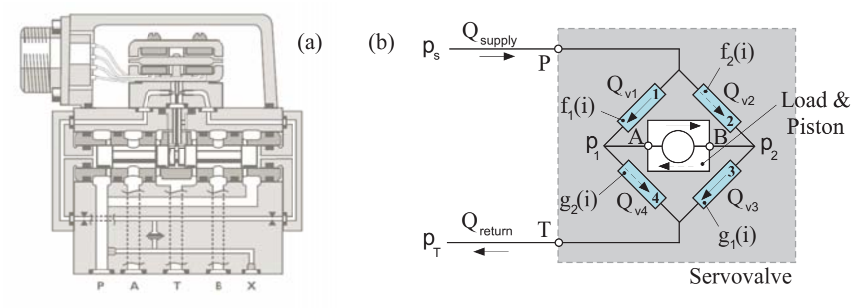

Figure 2. (a) A drawing of a real servovalve, (b) Schematic model of servovalve.

A good approximation is to assume that current functions are linear functions in the input current, when flow passes through the main path and constants, when flow passes through the leakage flow path. For instance, when $i > 0$, the main flow path passes through the orifices 1 and 3 and the functions are given by,

$$f_1(i) = K_1 i + K_{0,1}, \qquad f_2(i) = K_{0,2} \quad (6)$$

where K_1, $K_{0,1}$, and $K_{0,2}$ are positive constants, which correspond to the main and leakage valve flow path, and,

$$K_{0,1} = K_{0,2} \quad (7)$$

Further, neglecting leakages flows, the flows through the orifices of the servovalve described in Eqs. (4), are equal to the flows through the cylinder chamber ports, see Eq. (3a) and are written in the form

$$Q_{v1} = A_1 \dot{l}, \qquad Q_{v3} = A_2 \dot{l} \quad (8)$$

4 Invariant Error Dynamics Controller

To control the platform in operational (Cartesian) space, first, manipulator inverse kinematics is solved to transform motion requirements from operational-space into the joint-space. Then, an invariant error dynamics control scheme is designed that allows tracking of the reference inputs.

In electromechanical systems, the force acting on moving masses is proportional to actuator current. This simplifies their control laws and allows one to achieve second order error dynamics converging exponentially to zero. However, a simple relationship between force and current does not exist in electrohydraulic systems. Despite this, we are interested in studying whether such a system can be described by error dynamics such as

$$\ddot{\boldsymbol{e}} + \mathbf{K}_{\mathbf{v}}\dot{\boldsymbol{e}} + \mathbf{K}_{\mathbf{p}}\boldsymbol{e} = \mathbf{0} \tag{9}$$

where $\boldsymbol{e} = \boldsymbol{l}_{des} - \boldsymbol{l}$ is the 6×1 vector position error of the actuator displacements, $\boldsymbol{l}_{des}$ is the 6×1 desired vector of the actuator displacements, and $\mathbf{K}_{\mathbf{p}}$ and $\mathbf{K}_{\mathbf{v}}$ are 6×6 diagonal matrixes, which represent the control gains of the system and are given by,

$$\mathbf{K}_{\mathbf{p}} = \mathrm{diag}\{\omega_1^2, \omega_2^2, ..., \omega_6^2\}, \quad \mathbf{K}_{\mathbf{v}} = \mathrm{diag}\{2\zeta_1\omega_1, 2\zeta_2\omega_2, ..., 2\zeta_6\omega_6\} \tag{10}$$

where $\omega_j, \zeta_j, j=1,2,...,6$ are the closed-loop natural frequency and the critical system damping respectively, for the six linear actuators.

Using Eqs. (4), (6) and (8), the servocylinder chamber pressures are computed,

$$p_1\big|_j = [p_s - \frac{A_1^2}{(K_1 i + K_{0,1})^2}\cdot\dot{l}^2]\Big|_j, \quad p_2\big|_j = [p_T + \frac{A_2^2}{(K_1 i + K_{0,1})^2}\cdot\dot{l}^2]\Big|_j, \quad j=1,2,...,6 \tag{11}$$

Substituting Eqs. (11) into Eq. (3b), the hydraulic forces of the servoactuators are computed as,

$$[p_1 A_1 - p_2 A_2]\big|_j = [A_1 p_s - A_2 p_T - \frac{A_1^3 + A_2^3}{(K_1 i + K_{0,1})^2}\cdot\dot{l}^2]\Big|_j, \quad j=1,2,...,6 \tag{12}$$

In Eq. (12), i_j is the control input for the j[th] valve/ actuator and $[p_1 A_1 - p_2 A_2]\big|_j$ is the resulting actuator force. However, Eq. (12) is also function of the velocity of the actuators, $\dot{l}_j$. Substituting Eq. (12) in the system equation of motion, see Eqs. (1) - (2), the following equations of motion are derived,

$$\mathbf{M}(\boldsymbol{l})\ddot{\boldsymbol{l}} + \boldsymbol{V}(\boldsymbol{l},\dot{\boldsymbol{l}}) + \boldsymbol{G}(\boldsymbol{l}) + \boldsymbol{F}_{fr}(\dot{\boldsymbol{l}}) = \begin{bmatrix} [A_1 p_s - A_2 p_T - \frac{A_1^3 + A_2^3}{(K_1 i + K_{0,1})^2}\cdot\dot{l}^2]\Big|_1 \\ \cdots \\ [A_1 p_s - A_2 p_T - \frac{A_1^3 + A_2^3}{(K_1 i + K_{0,1})^2}\cdot\dot{l}^2]\Big|_6 \end{bmatrix} \tag{13}$$

Solving Eq. (13) for the input commands, i_j, $j=1,2,...,6$, the components of the servovalve current vector $\boldsymbol{i}=\begin{pmatrix} i_1 & i_2 & ... & i_6 \end{pmatrix}^{\mathrm{T}}$ are computed as,

$$i_j = \left[\frac{\dot{l}}{K_1 \sqrt{\frac{1}{A_1^3 + A_2^3} [A_1 p_s - A_2 p_T - \langle \mathrm{F} \rangle]}} - \frac{K_{0,1}}{K_1} \right] \Bigg|_j , \qquad j = 1,2,...,6 \tag{14}$$

where $\langle \mathrm{F} \rangle \big|_j$ represents the j element of the vector $\mathbf{M}(\boldsymbol{l})\ddot{\boldsymbol{l}} + \boldsymbol{V}(\boldsymbol{l},\dot{\boldsymbol{l}}) + \boldsymbol{G}(\boldsymbol{l}) + \boldsymbol{F}_{fr}(\dot{\boldsymbol{l}})$.

Further, assuming that Eq. (9) has been satisfied, this equation is solved for $\ddot{\boldsymbol{l}}$ which is substituted in the elements $\langle \mathrm{F} \rangle \big|_j$. Then, these elements are obtained,

$$\langle \mathrm{F} \rangle \big|_j = [\mathbf{M} \cdot (\ddot{\boldsymbol{l}}_{des} + \mathbf{K}_{\mathrm{v}} \dot{\boldsymbol{e}} + \mathbf{K}_{\mathrm{p}} \boldsymbol{e}) + \boldsymbol{V} + \boldsymbol{G} + \boldsymbol{F}_{fr}] \big|_j \tag{15}$$

Finally, the servovalve current vector, the elements of which are given in Eq. (14) describes the invariant error dynamics control law scheme for the 6-dof electrohydraulic Stewart platform. Note that the control law requires feedback of both the position and velocity length errors, as well as it includes the mechanism dynamics and a servovalve model.

Substituting Eq. (14) in Eq. (1), an equation of the form of Eq. (9) results, which demonstrates the stability of the system. The system control law is illustrated schematically in Figure 3.

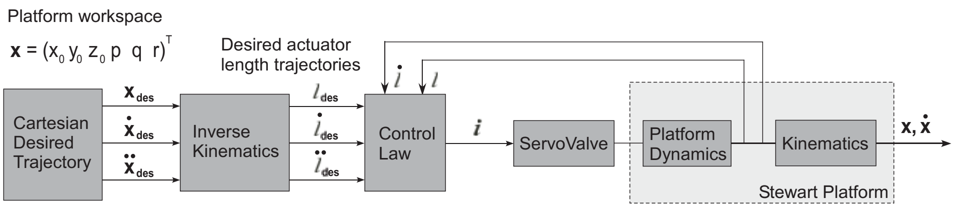

Figure 3. Schematic view of the invariant error dynamics controller diagram.

Simulation results. The tracking performance of the controller is evaluated on the servosystem, described by Eqs. (1) - (8), using Matlab/Simulink. The Cartesian desired trajectories of the platform cm are assumed to be

$$x_0(t) = x_c \sin(2\pi f t), \quad y_0(t) = y_c \cos(2\pi f t), \quad z_0(t) = z_{c1} + z_c \sin(2\pi f t) \tag{16a}$$

$$p(t) = p_c \cos(2\pi f t), \quad q(t) = q_c \sin(2\pi f t), \quad r(t) = r_c \sin(2\pi f t) \tag{16b}$$

where x_c, y_c, z_c, z_{c1}, p_c, q_c and r_c are trajectory constants.

Simulation runs were obtained using a number of desirable trajectories. As an example, Figure 4 and Figure 5 show typical results, in which the desired trajectories are given by Eqs. (16) with platform mass $m = 300\,kg$, moments of inertia about the center of platform mass of x, y, z axes $I_{xx} = I_{yy} = 25\,kgm^2$, $I_{zz} = 50\,kgm^2$, respectively, $f = 0.5\,Hz$, $x_c = 0.1\,m$, $y_c = 0.2\,m$,

$z_c = 0.1\,m$, $z_{c1} = 1.25\,m$, $p_c = 30^{\circ}$, $q_c = 20^{\circ}$, $r_c = 15^{\circ}$, $\omega_j = \pi$ *rad/s*, $\zeta_j = 1$ and friction parameters $b_j = 200\,\mathrm{Ns/m}$, $f_{C,j} = 20\,\mathrm{N}$, and $f_{s,j} = 50\,\mathrm{N}$, $j = 1, 2, ..., 6$. The platform displacements in the three Cartesian axes and orientation, and the position and orientation errors of the platform are shown in Figure 4. Also, one of the six leg lengths of the mechanism, the force acting on the platform, and the input signal for the same actuator, are depicted in Figure 5. The position errors converge to zero, as were expected, in settling time $t_{s,j} = 6/\omega_j\,[s]$, $j = 1, 2, ..., 6$. The remaining position errors of the steady state are due to the inertial forces caused by the harmonic trajectory.

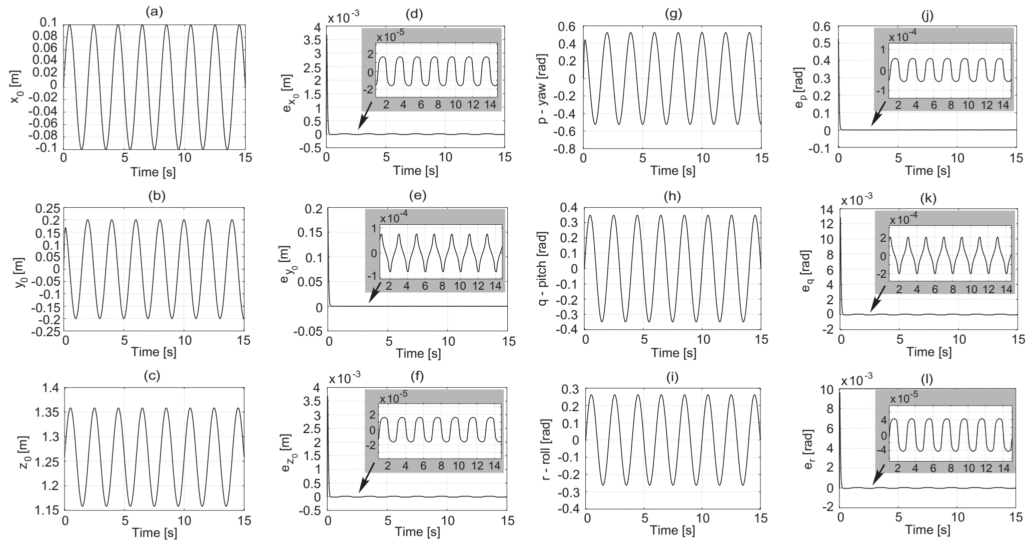

Figure 4. Simulation results. Platform displacement response, (a)-(c) and orientation, (g)-(i). Platform position errors, (d)-(f) and orientation errors, (j)-(l).

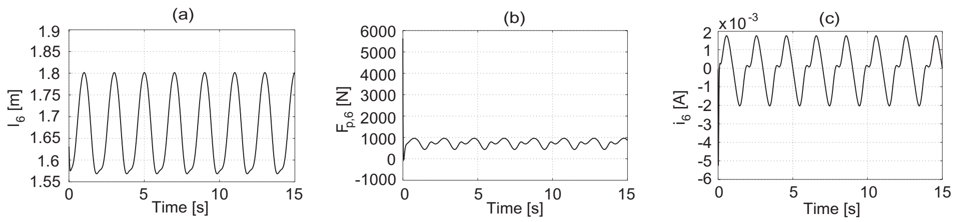

Figure 5. Simulation results. A servoactuator: (a) length position, (b) actuated force, (c) input signal.

5 Conclusions

This paper focused on the development of the invariant error dynamics controller for a 6-dof electrohydraulic Stewart platform. Rigid body and electrohydraulic models, which included servovalve dynamics and friction were employed. The developed controller employed the dynamic and hydraulic model of the system and yielded the six servovalve input current vector, in analytical form. Using mechanism inverse kinematics, the desired Cartesian trajectories yielded desired actuator length trajectories. Simulations with typical desired trajectories were presented and a good performance of the controller was obtained. The approach can be further extended to hydraulic manipulator and simulator control.

Bibliography

Stewart, D. (1965-66). A platform with six degrees of freedom. In *Proceedings of the IMechE,* Vol. 180, Pt. 1, No 15, 371–385.

Shim, J., H., Park, J., Y., Kwon, D., S., and Kim, S. (1997). Kinematic Design of a Six Degree-of-Freedom In-Parallel Manipulator for Probing Task. In *Proceedings of the IEEE Int. Conf. On Robotics and Automation,* New Mexico, 2967–2973.

Liu, M., J., Li, C., X., and Li, C., N. (2000). Generalized Stewart-Gough Platforms and Their Direct Kinematics. *IEEE Transactions on Robotics and Automation,* vol. 16, No. 1, 94–98.

Gao, X., S., Lei, D., Liao, Q., and Zhang, G., F. (2005). Generalized Stewart-Gough Platforms and Their Direct Kinematics. *IEEE Transactions on Robotics,* vol. 21, No. 2, 141–151.

Lebret, G., Liu, K., and Lewis, F., L. (1993). Dynamic Analysis and Control of a Stewart Platform Manipulator. *Journal of Robotic Systems,* 10(5), 629–655.

Tsai, L., W. (1999). Robot Analysis, The Mechanics of Serial and Parallel Manipulators. J. Wiley & Sons.

Tsai, L., W. (2000). Solving the Inverse Dynamics of a Stewart-Gough Manipulator by the Principle of Virtual Work. *Journal of Mechanical Design, Transactions of the ASME,* vol. 122, 3–9.

Li, D., and Salcudean, S., E. (1997). Modeling, Simulation, and Control of a Hydraulic Stewart Platform. In *Proceedings of the IEEE Int. Conf. on Robotics and Automation,* 3360–3366.

Sirouspour, M. R., and Salcudean, S. E. (2000). A New Approach to the Control of a Hydraulic Stewart Platform. *ISER 2000,* 447–460.

Kim, D., H., Kang, J., Y., and Lee, K., I. (2000). Robust Tracking Control Design for a 6 DOF Parallel Manipulator *Journal of Robotic Systems,* Vol. 17, No. 10, 527–547.

Merritt, H. E. (1967). Hydraulic Control Systems. J. Wiley.

Garagic, D., and Srinivasan, K. (2004). Application of Nonlinear Adaptive Control Techniques to an Electrohydraulic Velocity Servo-mechanism. *IEEE Trans. on Control Systems Tech.,* vol. 12, 303–314.

Sirouspour, M. R., and Salcudean, S. E. (2001). Nonlinear Control of Hydraulic Robots. *IEEE Transactions on Robotics and Automation,* vol. 17, No. 2, 173–182.

Honegger, M., and Corke, P. (2001). Model-Based Control of Hydraulic Actuated Manipulators. In *Proceedings 2001 IEEE Int. Conf. on Robotics & Automation*, Seoul, Korea, 2553–2559.

Davliakos, I., and Papadopoulos, E. (2005). Development of a Model-Based Nested Controller for Electrohydraulic Servos. In *Proceedings 13th Mediterranean Conference on Control and Automation,* June 27-29, Limassol, Cyprus, 107–112.

Nguyen, C., C., Antrazi, S., S., Zhou, Z., L., and Campbell, C., E. (1992). Adaptive Control of a Stewart Platform-Based Manipulator. *Journal of Robotic Systems,* 10(5), 657–687.

Kim, N., I., and Lee, C., W. (1998). High Speed Tracking Control of Stewart Platform Manipulator via Enhanced Sliding Mode Control. *IEEE Conf. On Robotics and Automation,* Belgium, 2716–2721.

Helouvry, B., A., Dupont, P., and De Wit, C., C. (1994). A Survey of Models, Analysis Tools and Compensation Methods for the Control of Machines with Friction. *Automatica,* 30: 7, 1083–1138.